International Journal of Greenhouse Gas Control 119 (2022) 103698

Contents lists available at ScienceDirect

International Journal of Greenhouse Gas Control

journal homepage: www.elsevier.com/locate/ijggc

Two-stage membrane cascades for post-combustion CO_2 capture using facilitated transport membranes: Importance on sequence of membrane types

Saravanan Janakiram [a,b], Arne Lindbråthen [a], Luca Ansaloni [b], Thijs Peters [b], Liyuan Deng [a,*]

[a] Department of Chemical Engineering, Norwegian University of Science and Technology (NTNU), Trondheim, NO 7491, Norway
[b] Department of Sustainable Energy Technology, SINTEF Industry, 0373 Oslo, Norway

ARTICLE INFO

Keywords:
Facilitated transport
CO_2 capture
Two-stage process
Recycle
Process simulation

ABSTRACT

The use of membrane module performance data obtained in industrially-relevant environment as the basis in process simulation can lead to a more realistic prediction of a CO_2 capture system. In this work, we report the use of two classes of industrially validated membranes, i.e., hybrid facilitated transport membranes (HFTMs), which are characterized by higher permeances and lower selectivity, and the fixed site carrier (FSC) polyvinylamine (PVAm) membrane, which is characterized by lower permeance and higher selectivity relative to each other, to study the potential of these membranes in two-stage configurations for post-combustion CO_2 capture applications. Two-stage cascades with and without recycle streams were simulated for a target CO_2 recovery of >80% and purity of 80–99.5%. Recycle systems were found to contribute in reaching high purity targets of CO_2 >90% at the fixed recovery of 90%. The positioning of membranes with different properties in different stages was found to influence the performance of the system significantly. Processes employing HFTMs in the first stage coupled with a PVAm membrane in the second stage performed best with the lowest total energy/membrane area requirement and recycle ratio for a target of 90% recovery and >90% purity of CO_2. The process employing HFTMs in both stages outperformed all other cases in terms of membrane area required. The case employing PVAm membranes in both stages performs at its optimum only at a lower purity requirement (<90%). This study reveals the importance of using an optimized combination of membranes with different separation capabilities at different stages.

1. Introduction

Membrane-based technologies are commercially used in various gas separation applications, including the production of nitrogen from air, separation of hydrogen from ammonia, and natural gas sweetening (Baker, 2004). The potential for membranes in CO_2 capture systems is increasingly explored with the development of high performance membrane materials with superior separation properties (D'Alessandro et al., 2010; S. Janakiram et al., 2020; Janakiram et al., 2019). Several strategies have been adopted to improve the permeation properties of membrane materials in polymeric membranes targeting efficient separation of feed streams with lean CO_2 concentration, typically for post-combustion flue gas (Park et al., 2017; Janakiram et al., 2018; Ahmadi et al., 2018; S. Janakiram et al., 2020). These improved membrane materials are characterized by very high CO_2 permeabilities and CO_2/N_2 selectivities, but often, not simultaneously. In lab-scale studies, the separation performance are usually reported as permeabilities in Barrer (1 Barrer $= 10^{-10}$ cm^3(STP) cm^{-1} s^{-1} cm $Hg^{-1} = 3.35 \times 10^{-16}$ mol m^{-1} s^{-1} Pa^{-1}) and ideal selectivities (ratio of pure gas permeabilities). However, such parameters refer to the properties of the bulk selective layer. In the cases where the materials are coated as thin film composite membranes (TFC) in the form of flat sheet or hollow fibers, the separation properties are reported as permeance (transmembrane flux) in GPU (1 GPU $= 10^{-6}$ cm^3(STP) cm^{-2} s^{-1} $cmHg^{-1} = 3.35 \times 10^{-10}$ mol m^{-2} s^{-1} Pa^{-1}) and separation factors (concentration-based selectivity). Performance evaluation of TFC membranes is closer to realistic membrane separation as they account for non-ideal phenomena related to the boundary layer (e.g., concentration polarization) as well as for the feasibility of coating ultra-thin selective layer, as required by the high permeance target in post combustion CO_2 capture applications.

* Corresponding author.
E-mail address: liyuan.deng@ntnu.no (L. Deng).

https://doi.org/10.1016/j.ijggc.2022.103698
Received 25 February 2022; Received in revised form 5 May 2022; Accepted 26 May 2022
Available online 3 June 2022

While lab-scale TFC membranes are typically tested in relatively small areas (in the order of cm^2), recently, many studies increasingly report performances of membrane modules on a larger scale (Y. Han et al., 2019; Z. Dai et al., 2019; Salim et al., 2018; White et al., 2015). Individual membranes sealed into modules at high packing density and surface area do not necessarily retain the same permeation properties (permeance and selectivity) as the bulk selective layer tested with a smaller area during lab-scale development (Li et al., 2004). The membrane module performance widely depends on a variety of parameters like stage-cut, flow patterns inside the module, and pressure drop, as well as boundary layer effects (Glenn Lipscomb and Sonalkar, 2004). Additionally, the scaled-up modules are tested in actual industrial conditions, which also elicit changes in feed streams and operational environment.

There exist numerous studies that prove the potential of membranes in CO_2 capture applications through simulations and optimizations (Giordano et al., 2017; Ho et al., 2008; Belaissaoui et al., 2012; Shao et al., 2013; Franz et al., 2013; He et al., 2015). Nevertheless, in most cases, hypothetical or extrapolated permeances calculated from permeability data obtained from a labscale evaluation are commonly used as the basis of simulations. Many simulation studies also involve changing operating conditions including pressure and temperature, which in fact influence separation properties significantly. Such deviations are unfortunately usually ignored in most studies. Only a handful of these studies report simulation results using membrane permeance data validated in an industrially relevant pre-pilot scale or at even larger scale. Franz et al. studied the effect of sweep gas on a cascaded membrane process in a reference scale of 600 MW power plant using permeance data of commercial PolyActive membrane modules (Franz et al., 2013). Low et al. used PVAm/PVA facilitated transport and thermally rearranged PBI membranes to study the effect of humidity on CO_2 separation using a flue gas capacity of 100 $Nm^3\ h^{-1}$ (Low et al., 2013). He et al. used pilot scale data of fixed site carrier polyvinylamine membrane to perform a feasibility analysis for a >80% CO_2 capture ratio and >95% CO_2 purity using 18,260 kmol/h flue gas in a refinery (He et al., 2015). All such simulation studies consistently have to employ a multi-stage cascade system to reach the target of a high CO_2 purity and CO_2 recovery. Until now, however, no studies have reported the use of membranes with different properties in the different stages in such multi-stage systems.

The present study investigates cases of membrane-based separation cascades using industrially validated membranes in different stages to achieve overall capture rate and CO_2 purity targets. The study simulates a two-stage membrane process using two class of membranes in different stages – Hybrid Facilitated Transport Membrane (HFTM) characterized with high permeances and low selectivity and Fixed Site Carrier (FSC) polyvinylamine (PVAm) membrane characterized with low permeance and high selectivity relative to each other. The separation performance of these membranes obtained in an industrial environment were used as the basis for the simulation study (He et al., 2017; Sandru et al., 2013; Kim et al., 2013; Janakiram et al., 2021). The influence of different properties of the membranes in different stages on the overall separation performance in a two-stage system has been systematically studied elucidating the advantages of smart positioning of membranes for lowering the total membrane area and energy requirement.

2. Simulation basis

The process simulations in this study were carried out in Aspen HYSYS V9.0 interfaced with an in-house customized membrane model ChemBrane. Detailed information about Chembrane can be found in previous studies (Grainger and Hägg, 2008; Grainger, 2007). ChemBrane is a user operation module that uses a successive stage model to solve for flux in a mixed gas feed operated in counter-current mode. The ChemBrane model assumes a constant permeance across the membrane module.

A pilot scale sizing of 50 $Nm^3\ h^{-1}$ of flue gas was arbitrarily chosen as a basis feed flow for simulations to compare different configurations. The motivation behind using pilot-scale sizing is because the analysis in this study is limited to membrane area and total energy requirement, which scale linearly with respect to feed flow. The composition of the feed on dry and wet basis is summarised in Table 1, which reflects a typical cement industry case (Psarras et al., 2017).

2.1. Description of assessed process configurations

Two two-stage cascade process configurations were studied with membrane-based systems in this study. Fig. 1 shows the outline of the two-stage membrane cascade, where the purification of the permeate stream from the first stage is performed using a second stage membrane process without recycle stream (I) and with recycle stream (II).

As water plays a crucial role for permeation in facilitated transport membranes, fluctuations in the humidity of the feed stream will widely affect the transport properties of the membrane material (Deng and Hägg, 2010; Hägg et al., 2017). Hence, a dedicated feed humidifier was considered as a part of the process after feed compression, which ensures the input stream to the membrane is humidified to 95% RH at 60 °C. Moreover, according to the well-accepted facilitated transport mechanism (He et al., 2015), the water permeability in this type of membranes is usually high, leading to a water saturated permeate stream and a rather dry retentate stream. Hence, in this work, the second stage membrane purification was applied only on the permeate stream of the first stage to avoid any re-humidification of gas streams. It has to be noted that the constant permeance has been used to avoid complexity of changing permeances with depleting water concentration along the length of module (Belaissaoui et al., 2020). However, the availability of typical flue gas at point sources at near saturation conditions when used in modules of shorter length reduces the deviation of permeation performances inside the module.

The feed pressure was maintained at 1.7 bar in the first stage in both processes. Typical flue gas streams vary widely in terms of CO_2 composition. Often, feed compression is used to increase the driving force and achieve enhanced separation due to higher CO_2 partial pressures. However, it should be noted that compression of feed might lead to a critically high share of energy consumption, since 60–90% of the non-CO_2 components constitute the flue gas. Alternatively, vacuum was used in the permeate side of the membrane in both stages in this work for two main reasons – to increase the driving force for gas transport across the membranes and maximize the pressure ratio (ratio of feed pressure to permeate pressure) in order to enhance separation capability of the membrane stage. The permeate pressure was maintained at 100 mbar in both stages using vacuum pumps (Y. Han et al., 2019). All membrane units were operated at 60 °C. This temperature was used to match the field test conditions in which the membranes were validated.

The permeate stream in the first stage is recompressed and fed to the second stage module. The high water permeance of the FTM membranes used in the first stage eliminates the need for a secondary humidification unit. The interstage compression was varied between 1.7 bar and 10 bar in Process I and maintained at a constant value of 1.7 bar in Process II. The retentate of the first stage is mixed with second stage retentate in Process I at the same pressure before releasing and is released at 1.7 bar in Process II.

Table 1
Flue gas composition used in the simulation study (Gas at 60 °C).

Component	Mole fraction	
	dry basis	wet basis
CO_2	0.17	0.15
N_2	0.68	0.59
O_2	0.15	0.13
H_2O	0.00	0.13

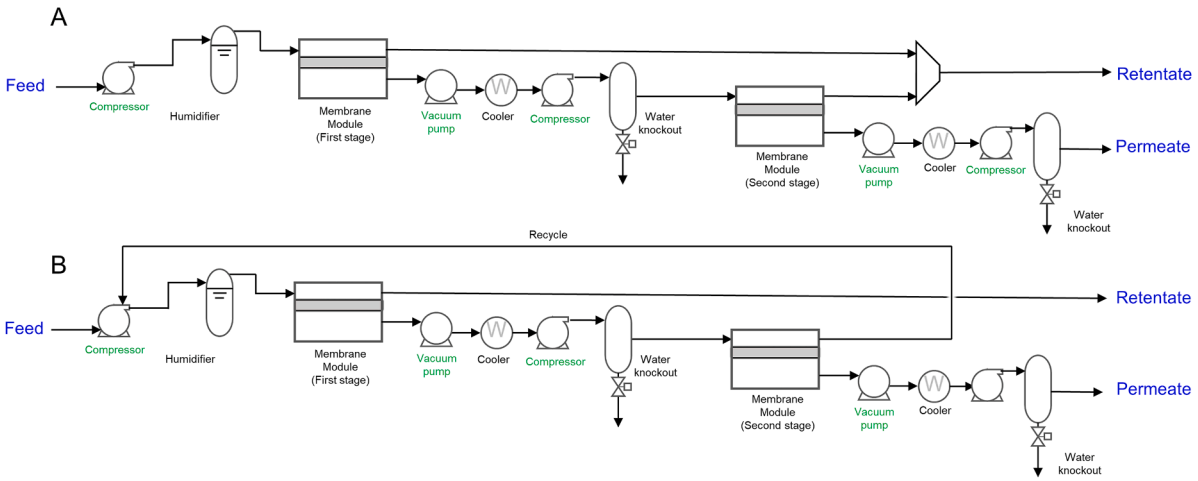

Fig. 1. Process flow diagrams of the simulated two-stage post combustion capture plant without recycle stream (I) and with recycle stream (II).

The permeate stream of the second stage is recompressed to 1.05 bar and cooled down to 30 °C. The dry CO_2 mole fraction of the cooled permeate stream is reported as the CO_2 purity (%). The retentate stream is cycled back to the feed compressor in the case of Process II.

2.2. Membrane materials

Four case scenarios were considered in each of the two process configurations. A total of three membranes were investigated for individual stages:

- HFTM based on SHPAA/PVA (sterically hindered polyallyl amine/polyvinyl alcohol)blend containing 0.2 wt% porous GO (S. Janakiram et al., 2021; S. Janakiram et al., 2020).
- HFTM+ProK containing a mobile carrier 20% ProK (Potassium salt of Proline) in addition to 0.2 wt% porous GO in the SHPAA/PVA blend (S. Janakiram et al., 2021; S. Janakiram et al., 2020).
- FSC - PVAm membrane previously developed at NTNU and tested and validated at Technology Readiness Level (TRL) of 6.

The HFTM exhibits a module selectivity of ~20, while the HFTM+ProK exhibits a lower selectivity (~16) albeit a higher CO_2 permeance (25% higher than that of the HFTM) (S. Janakiram et al., 2020). Both HFTM's are characterised by high permeances (Table 2). FSC PVAm membranes offer high selectivity (~86), while its permeance is around one order of magnitude lower than the HFTM membranes. The gas permeance values for each membrane are provided in Table 2.

With two process configurations and three membrane types, a total of eight case scenarios were studied in this work. Naturally, in most cases, HFTMs were used in the first stage (due to the high permeance) followed by the PVAm membrane in the second stage (due to high selectivity). A base scenario (case A, PVAm membranes in both stages) was also studied to benchmark the HFTM's. The summary of these case scenarios is presented in Table 3.

The permeance data of all the membranes used in these simulations were validated experimental data (S. Janakiram et al., 2021; Hägg et al., 2017; S. Janakiram et al., 2020). The permeance values of gas components for each HFTM were obtained by manually adjusting and matching (Trial and error approach) of the relative ratios with ChemBrane in Aspen HYSYS V9.0, so that the simulated compositions of streams matched with the gas compositions measured in the exit permeate and retentate streams during the field tests for the same membrane area (S. Janakiram et al., 2021).It must be noted that these permeance values have not been analysed for changes with respect to operating conditions like feed pressure and temperature. This limitation justifies the use of a fixed feed pressure of 1.7 bar and temperature of 60 °C to match with the experimental conditions used in determination of permeances.

In the case of PVAm membrane, the permeances were adopted from the reported data from our prior studies (He et al., 2017; Sandru et al., 2013; Kim et al., 2013). Unlike HFTMs, the permeance of PVAm membranes have been studied for a wider range of operational pressure and hence, the use of higher interstage pressure especially in the cases where the PVAm membrane is used in the second stage is justified.

Table 2
Summary of permeation data used.

Membrane type	Permeance* (x 10^5 mol m^{-2} kPa^{-1} s^{-1})			
	CO_2	Nitrogen	H_2O	Ref
PVAm	4.89	0.06	9.17	(He et al., 2017; Sandru et al., 2013; Kim et al., 2013; Hägg et al., 2017)
HFTM	38.33	1.92	191.67	(S. Janakiram et al., 2020)
HFTM+ProK	48.06	2.97	239.72	(S. Janakiram et al., 2020)

*Permeation data measured at 60 °C/78% RH feed at 1.7 bar/vacuum 0.2 bar using raw flue gas from cement plant. Permeation data for PVAm obtained in pilot facility at NORCEM at 39 °C saturated feed at 3.3 bar/vacuum 0.2 bar using raw flue gas from cement plant (Hägg et al., 2017).

2.3. Assumptions

The following assumptions were made in the simulation study.

- Adiabatic efficiency of compressors and vacuum pumps is modelled at 75%.
- Vacuum pump is modelled as a compressor.
- No pressure drop was considered over the membranes.
- Total energy consumption of the process is the sum of power required for (i) feed compression/recompression and (ii) vacuum pump in both stages.
- Only single stage compression or suction was used for the sake of simplicity. Compressed streams were cooled to the required

Table 3
Summary of simulated process cases.

Two-stage configuration	Stages	Case A	Case B	Case C	Case D
Without recycle	1st	PVAm	HFTM+ProK	HFTM+ProK	HFTM
	2nd	PVAm	HFTM	PVAm	PVAm
With recycle	1st	PVAm	HFTM+ProK	HFTM+ProK	HFTM
	2nd	PVAm	HFTM	PVAm	PVAm

temperature using a cooler powered by cooling water. The cooling water was assumed to be freely available and hence, the cooler energy is not accounted in total energy of the process.
- The permeance data of PVAm and HFTM were assumed to be independent of feed pressure.

3. Results and discussion

3.1. Two-stage process without recycle

Typical post-combustion flue gas capture processes target both a high purity and high capture rate of CO_2 simultaneously. The CO_2 capture rate or CO_2 recovery is the ratio of CO_2 in the permeate relative to that of the feed. An optimistic target for the CO_2 recovery is 80–95% coupled with a high CO_2 purity of over 95% (Wang et al., 2017; Zhao et al., 2010). It should also be noted that the development of CO_2 utilization technologies is continuously driving changes in industrial requirements towards reduced CO_2 purity targets and at times recovery targets (Zhaurova et al., 2021; Ghiat and Al-Ansari, 2021). Nevertheless, for membrane-based processes, targets over 80% CO_2 purity with 80–95% CO_2 recovery are unreachable by using a single stage system due to a very high membrane selectivity requirement for a given nominal operation pressure ratio (Favre, 2007; Yang et al., 2009). A two-stage membrane process is therefore required to further purify the permeate stream at the same or higher-pressure ratio while thereby compensating for the high selectivity requirement in a single stage. However, for a fixed pressure ratio in each stage, the obtainable purity of CO_2 at a given fixed overall capture ratio is still a function of the membrane transport properties. Herein, the effect of membrane transport properties in a two-stage cascade operated at similar conditions is studied for four cases (A, B, C and D) that combine membranes of different characteristics in varying order. When the pressure ratio is set at 17 for both stages (feed pressure at 1.7 bar and permeate side vacuum at 0.1 bar), for a fixed capture ratio of 90%, the achievable CO_2 purity of the different cascades were evidently dependent on the membrane characteristics and their order of placement as seen in Fig. 2. In order to investigate the effect of increasing driving force in the second stage targeting higher overall capture performance, the interstage feed pressure was varied from 1.7 bar to 10 bar. The base case A employing a low-permeability, high selectivity membrane in both stages results in a surprisingly low CO_2 purity (82–83%). On the other hand, case B with two of the HFTMs (with relatively low selectivity but high permeability compared to the PVAm membrane) exhibited the lowest CO_2 purity of around 76–79% within the range of interstage feed pressure studied. The combination of high flux membranes (HFTM+ProK) followed by high selectivity PVAm membrane in the second stage had the highest achievable CO_2 purity of about 85% at a CO_2 recovery of 90%. When the CO_2 capture ratio was reduced to 80%, the achievable CO_2 purity increased by about 5% in all cases while preserving the same trend with respect to combinations on the achievable purity. The maximum achievable CO_2 purity with the best case (case C) was 89.4% with an interstage pressure of 10 bar. Interestingly, the effect of the interstage feed pressure on CO_2 purity is not significant. The increment in CO_2 purity is only 2–3% when increasing the interstage feed pressure from 1.7 to 10 bar, and most of which is in the range of 1.7 to 2.0 bar.

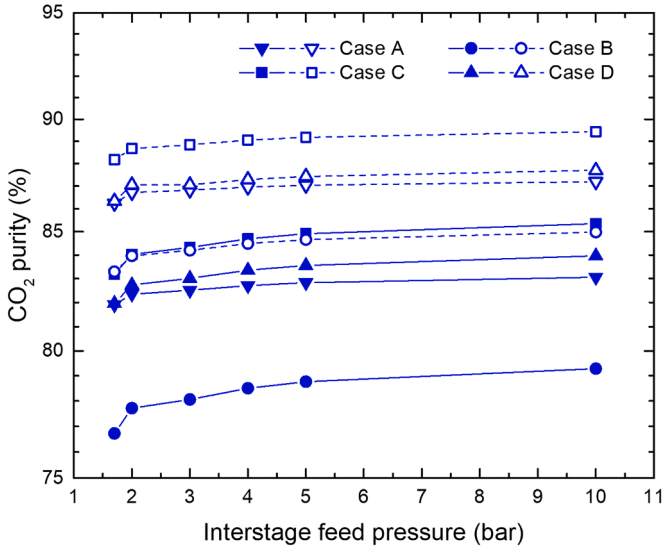

Fig. 2. CO_2 purity as a function of interstage pressure for a fixed CO_2 recovery of 80% (empty symbols connected with dotted lines) and 90% (filled symbols connected with solid lines) for 50 $Nm^3\ h^{-1}$ of feed flue gas in two-stage system without recycle (feed pressure in stage 1 = 1.7 bar; interstage pressure = 1.7–10 bar; permeate side: 0.1 bar vacuum in both stages; T = 60 °C).

Fig. 3 presents the influence of CO_2 purity on total membrane area and energy requirement for a fixed CO_2 recovery of 80% and 90%. In each case, the interstage pressure is varied from 1.7 bar to 10 bar to result in the required CO_2 purity. As it can be seen, at higher required CO_2 purity, the total membrane area required showed a reducing trend in most cases making it advantageous to utilize the second stage membrane at a higher driving force by increased interstage compression (Fig. 3A and B). However, it should be noted that the added compression in the interstage also results in significantly higher energy penalty and the relevant investment. Hence, with increasing purity, more energy is spent on the second stage, as shown in Fig. 3. Case B operated at lower CO_2 purity range at the considered range of interstage pressures owing to the low selectivity of the membrane following compression. On the other hand, cases A, C and D showed similar trends in membrane area and energy requirement for higher purity targets.

It can also be seen that the combinations employing HFTMs in stage 1 (Case B, C and D) require the least membrane area for separation and the combination of PVAm in stage 1 (Case A) require the most. However, such differences were hardly observed in the total energy requirement (between 5 and 9 kW for all cases).

Nevertheless, the limitations of a two-stage cascade were apparent with respect to the maximum achievable target CO_2 purity, which was below 90% for all the cases considered, even with a high interstage compression of 10 bars. It should also be noted that facilitated transport membranes suffer carrier saturation phenomenon with changing permeances and selectivity upon increasing feed pressure, which could further influence the system performance in terms of membrane area required (S. Janakiram et al., 2020; Z. Dai et al., 2019; Helberg et al., 2021). However, due to complexity of the changing performances and the relatively smaller size of second stage of membrane (less influence in total membrane area), constant performances in second stages were assumed. On the energy front, the feed compression in the first stage makes stage 1 more energy intensive due to the large volumetric flow. Another alternative that can be used without increasing the number of stages is recycling of retentate stream of stage 2 back to the feed stream of stage 1. This approach is investigated in the following section.

3.2. Two-stage process with recycle stream

Given that the achievable CO_2 purity of the two-stage process was limited to less than 90% without a significant increase in the pressure ratio in both membrane stages, an alternative solution consisting of recycling the retentate stream of stage 2 back to the feed stream was considered. The use of recycle streams has been widely reported in two-stage membrane cascades to reach the purity target while simultaneously ensuring the recovery, which can also enhance the driving force for permeation in the first stage because of the relatively high CO_2 concentration in the recycled stream (Deng and Hägg, 2010; Yang et al., 2009). Recycling streams particularly prove beneficial in low CO_2 content flue gases. However, it has to be noted that the volumetric flow to

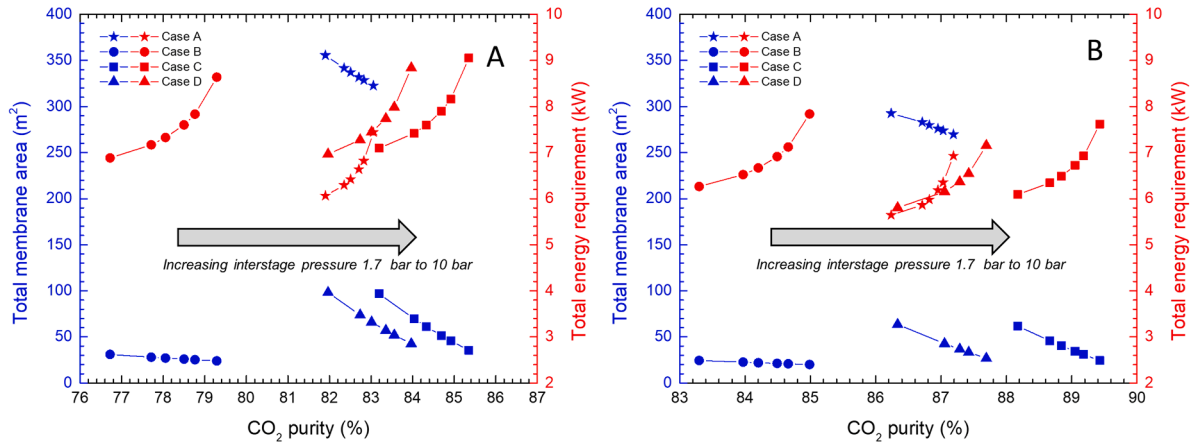

Fig. 3. Influence of CO_2 purity on total membrane area and energy requirement for a fixed CO_2 recovery of (A) 80% and (B) 90% for 50 $Nm^3\ h^{-1}$ of feed flue gas in two-stage system without recycle. (Feed pressure in stage 1 = 1.7 bar; Interstage pressure = 1.7–10 bar (increasing left to right in each dataset; Permeate side: 0.1 bar vacuum in both stages; T = 60 °C.).

the modules is increased by recycling, which is expected to increase the sizing of the equipment and energy consumption. Similar to the previous process, four cases of the same arrangement as mentioned in Table 2 were analysed in the process with recycle. The CO_2 recovery was fixed at 90% for all cases and the CO_2 purity ranging from 80% to 99.5% was set as the simulation target. Since no changes in pressure ratio in both the stages were considered in these simulations, the permeance values used correlate to calculated experimental values and, therefore, are expected to be closer to real separation outcomes.

3.3. *Influence of targeted CO_2 purity on required recycle ratio*

An important parameter for consideration in a recycle system is the recycle ratio, which is the ratio of the volumetric flow of the recycle stream to that of the feed stream. In general, a larger recycle ratio results in a higher output purity, but also leads to a higher energy penalty for the overall system. Hence, for a fixed capacity, the lowest possible recycle ratio is often preferred to achieve the target separation. Fig. 4 presents the recycle ratio requirement for the different cases considered in order to achieve a particular target CO_2 purity. In all the considered cases, up to 95% purity in CO_2 was achieved with a recycle ratio of less than 1. For a purity greater than 95%, the required recycle ratio increased rapidly as expected.

Interestingly, the recycle ratio required to reach a target purity depends also on the membrane placement as seen in Fig. 4. For the same target purity, Case A required the least recycle ratio for up to ~90% purity in the exit stream (yellow region). When the purity is above 90%, Cases C and D with high permeance membranes in Stage 1 and high selectivity membranes in Stage 2 cross over and become more promising (green region). For instance, for a target CO_2 purity of 87%, Case A requires a recycle ratio of 0.16, while cases C and D require ~0.21 for the same purity. However, at a high purity target of 95%, Case A require a

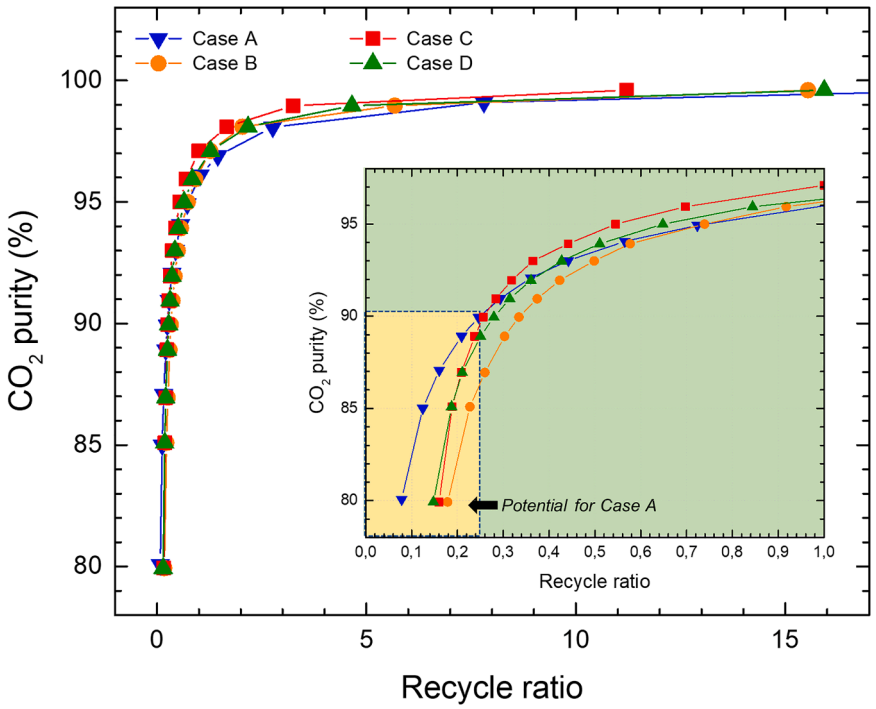

Fig. 4. Influence of targeted CO_2 purity on required recycle ratio for a fixed CO_2 recovery of 90% for 50 $Nm^3\ h^{-1}$ of feed flue gas (Feed pressure in stage 1 = 1.7 bar; Interstage pressure = 1.7 bar; Permeate side: 0.1 bar vacuum in both stages; T = 60 °C.).

recycle ratio of 0.72 while cases C and D of 0.55 and 0.65, respectively. Case B with (low selectivity membranes on both stages) require the highest recycle ratio across most of the range considered.

3.4. Influence of targeted CO_2 purity on total energy requirement

The total energy requirement for the targeted CO_2 purity ranging from 80% to 99.5% was also analysed for all cases and the results are presented in Fig. 5. As expected, the use of membranes with low selectivity in both stages result in a high recycle ratio requirement. Consequently, the associated vacuum pump and compressor load result in a higher energy requirement and the increase becomes exponential for purities in excess of 95%. Similar trends are observed in total energy requirement for Cases C and D with respect to the Case A. Two regions are identified; for a CO_2 purity of up to ~90% (yellow region), Case A require the least energy, and above that, Cases C and D require the least energy (green region).

3.5. Influence of membrane positioning

While the influence of membrane selectivity was apparent both on the recycle ratio and the total energy requirement, the permeation properties of membranes used in both stages was also found to largely influence the total membrane area required, as seen in Fig. 6. For the same target of CO_2 purity, Case A requires the most area and Case B requires the least as expected, since membranes in both stages of case B have the highest CO_2 permeance while in Case A have the lowest. The area requirements of Cases C and D (which combine high permeance and selectivity membranes) are in between those of Cases A and B. Although the total membrane area requirement increases for very high CO_2 purity targets (> 95%), interestingly, for Cases C and D the total membrane area decreases with increasing CO_2 purity to up to about the CO_2 purity of 95%, and then increases sharply when above 95%. In Cases A and B, the required membrane area increases steadily first, but the increase becomes more drastic above the CO_2 purity of 95%.

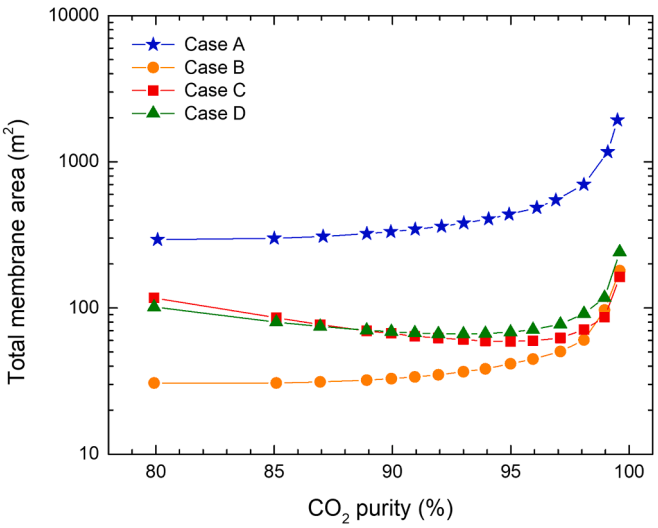

Fig. 6. Influence of CO_2 purity on total membrane area requirement for a fixed CO_2 recovery of 90% for 50 $Nm^3\ h^{-1}$ of feed flue gas. (Feed pressure in stage 1 = 1.7 bar; Interstage pressure = 1.7 bar; Permeate side: 0.1 bar vacuum in both stages; T = 60 °C.).

In order to explain the interesting trends of cases C and D that exclusively employ the high selectivity membrane in the 2nd stage, cases A, C and D were further analysed to study the interrelation of membrane properties between different stages. Fig. 7 shows the decoupled membrane area requirement for each stage. The membrane area for stage 1 increases with increasing CO_2 purity targeted. On the other hand, the membrane area for stage 2 decreases more rapidly for Cases C and D relative to Case A. Hence, the total area requirement, although governed mainly by stage 1, is largely influenced by stage 2 up to the purity target of 95%. Above 95%, a large area requirement in stage 1 seems to have

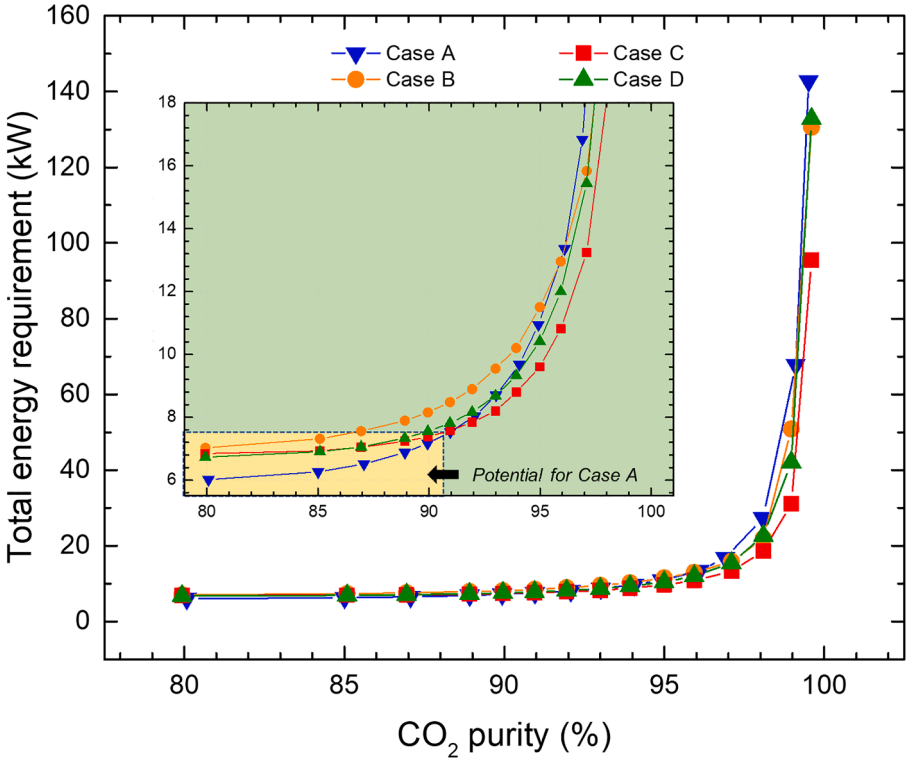

Fig. 5. Influence of CO_2 purity on total energy requirement for a fixed CO_2 recovery of 90% for 50 $Nm^3\ h^{-1}$ of feed flue gas. (Feed pressure in stage 1 = 1.7 bar; Interstage pressure = 1.7 bar; Permeate side: 0.1 bar vacuum in both stages; T = 60 °C.).

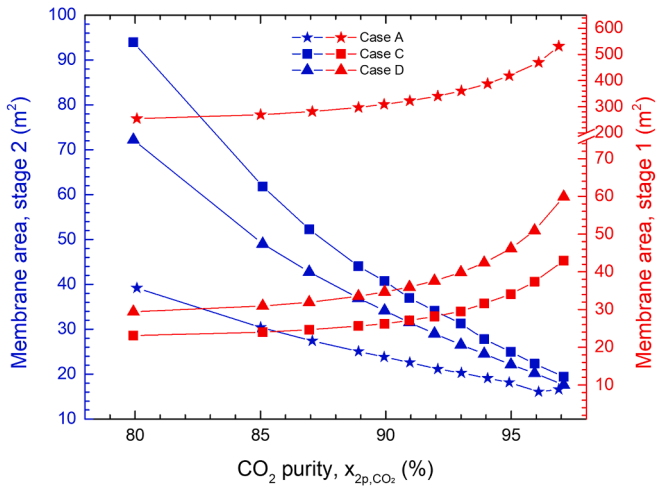

Fig. 7. Influence of target CO_2 purity on membrane area requirement in each stage for different CO_2 purity targets with a fixed CO_2 recovery of 90% for 50 $Nm^3\ h^{-1}$ of feed flue gas. (Feed pressure in stage 1 = 1.7 bar; Interstage pressure = 1.7 bar; Permeate side: 0.1 bar vacuum in both stages; T = 60 °C.).

counterweighed the effect of the decreasing trend in stage 2 on the overall membrane area. Nevertheless, the membrane area requirement behavior for stage 2 as function of CO_2 purity is distinctly different for Cases C and D.

In general, for a two-stage cascade, the CO_2 recovery is governed by first stage while the second stage guides the CO_2 purity of the final permeate stream. However, with the presence of recycle, the second stage membrane can operate at varying conditions depending on the size and concentration of the recycle stream (extra degree of freedom). In the current analysis, since in the considered cases A, C and D, the membrane type is the same in the second stage, it can be hypothesized that the different behavior of stage 2 is caused by the different separation performance and hence the retentate composition of stage 1. The membrane area requirement in stage 2 is directly related to the separation by the first membrane stage. In other words, the required area for a particular purity target is dependent on both the flow and concentration of CO_2 in the feed to the second stage. Clearly, the feed to the second stage contains higher concentration of CO_2 ($x_{2f,\ CO_2}$) in Case A than in Case C and D, as seen in Fig. 8A. This is explained by the high selectivity of the membrane employed in the first stage in Case A. However, this high CO_2 concentration in the feed causes the second stage membrane in Case A to operate at a higher average feed concentration range where the ratio of retentate to feed CO_2 concentration ($x_{2r,\ CO_2}$ /$x_{2f,\ CO_2}$) dominates the average driving force on the module.

This phenomenon can be explained by aid of the cross-flow model for a gas separation module (Mulder, 1996). A cross-flow model can be used as an analogue to a module operated in counter-current configuration with vacuum on the permeate side.

$$x_{2p,\ CO_2} = B - \left[B^2 - \left(\frac{\alpha}{(\alpha-1)\varphi}\right)\bar{x}_{2f,\ CO_2}\right]^{0.5} \quad (1)$$

$$\bar{x}_{2f,\ CO_2} = \frac{x_{2f,\ CO_2} - x_{2r,\ CO_2}}{ln\left(\frac{x_{2f,\ CO_2}}{x_{2r,\ CO_2}}\right)} \quad (2)$$

$$B = 0.5.\left[1 + \frac{1}{(\alpha-1)\varphi} + \frac{\bar{x}_{2f,\ CO_2}}{\varphi}\right] \quad (3)$$

where$\bar{x}_{2f,\ CO_2}$ is the log mean feed CO_2 concentration, $x_{2p,\ CO_2}$ is the required CO_2 purity (permeate CO_2 concentration), $x_{2r,\ CO_2}$ is the second stage retentate concentration of CO_2 (same as the recycle stream), α is the membrane selectivity, and φ is the pressure ratio defined as

$$\varphi = \frac{P_p}{P_f} \quad (4)$$

where P_f and P_p are the feed and permeate pressures.

In the analyzed systems, since the pressure ratio ϕ and membrane selectivity remain constant for Cases A, C and D, the coefficient B defined in Eq. (3) is sensitive to the log mean average CO_2 concentration in the feed, $\bar{x}_{2f,\ CO_2}$. $x_{2p,\ CO_2}$ is a solution to quadratic equation with opposing functions relating to $\bar{x}_{2f,\ CO_2}$and how it changes after treatment from the first stage.

From Eq. (2), the log mean upstream concentration in stage 2 depends both on the magnitude of individual concentrations of the feed and retentate, as well as their ratio. As the ratio between $x_{2r,\ CO_2}$ to $x_{2f,\ CO_2}$ increases, the load in terms of separation on the 2nd membrane stage increases because the log mean average feed concentration increases. Fig. 8B presents the influence of target CO_2 purity on average feed concentration of CO_2 in the second stage. As it can be seen, the profiling of $\bar{x}_{2f,\ CO_2}$is nearly linear with respect to target CO_2 purity in Case A, while for cases C and D, it changes with an increasing slope at each increasing CO_2 purity. The varying curvature is attributed to the log function and dependence on the ratio between $x_{2r,\ CO_2}$ to $x_{2f,\ CO_2}$, which shows a sigmoidal increase for cases C and D for increasing purity requirements. For a particular target purity, this ratio and eventually $\bar{x}_{2f,\ CO_2}$ is high for Case A relative to Cases C & D, and hence the last term

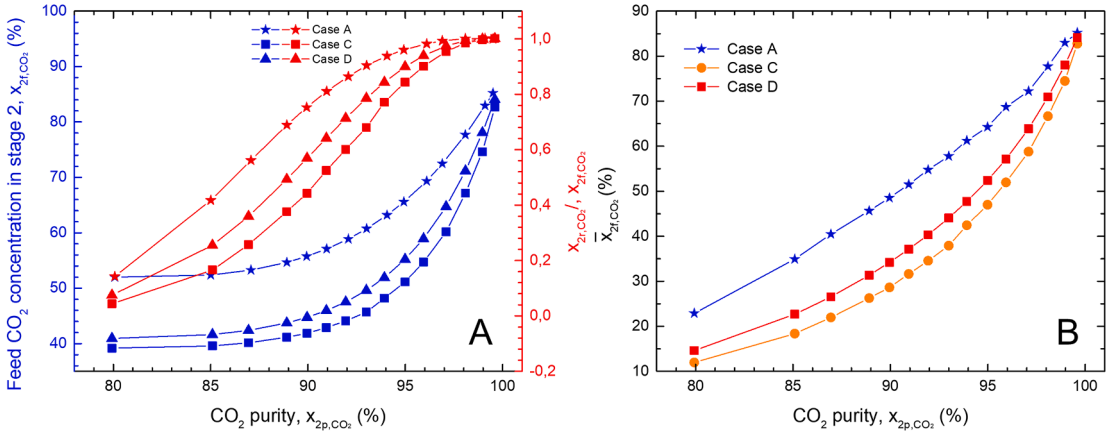

Fig. 8. (A) Change in $x_{2f,\ CO_2}$ and the ratio of $x_{2r,\ CO_2}$ to $x_{2f,\ CO_2}$ in stage 2 for different CO_2 purity targets (B) Influence of target CO_2 purity on average feed concentration of CO_2 in the second stage for a fixed CO_2 recovery of 90% for 50 $Nm^3\ h^{-1}$ of feed flue gas. (Feed pressure in stage 1 = 1.7 bar; Interstage pressure = 1.7 bar; Permeate side: 0.1 bar vacuum in both stages; T = 60 °C.).

in Eq. (2) becomes more significant for the value of coefficient *B*.

The main reason behind the changing separation conditions in stage 2 is the selectivity of the membrane in stage 1. From the analyzed data, a high inlet feed concentration of CO_2 to stage 2 obtained from stage 1 inflicts large penalties in terms of separation duty in stage 2, which is counterproductive in terms of both area and energy requirement, as seen from Figs. 5 and 6, respectively. While the current trend of energy and area requirement is valid for the membrane types and cascades considered, the presence of recycle stream adds to complexity in identifying the influence of individual operational parameters in a stage on the other stage due to simultaneous changes in different variables. Further studies are needed to explore these phenomena with more membranes of different separation properties and in different or multi-stage cascades.

Fig. 9 summarises the relative changes in total energy and membrane area requirement for cases C and D in contrast to Cases A across the entire range of CO_2 purity analysed. From Fig. 9, it is apparent that the use of a less selective membrane in the first stage is beneficial in terms of both energy and membrane area required for the ranges of CO_2 purity over 90%. On the other hand, using a high selective membrane only in the second stage for higher purification is beneficial in terms of energy requirement when compared to using low selectivity membranes in second stage as seen in Fig. 10. However, if the target requirements to reach industrial needs are low, case B offers the least total area requirement across the entire range of CO_2 purity requirement, owing to the high permeances offered in both stages.

Nevertheless, the use of a highly selective membrane in both stages in a two-stage recycle system can be less beneficial, let alone the large area requirement to compensate for the lower permeability of the membranes. Case C with a high permeable, low selective membrane in the first stage followed by a high selectivity, low permeable membrane in the second stage in a two-stage system with recycle yields a simultaneous low total membrane area requirement, low recycle ratio and low total energy requirement for a 90% recovery and >90% purity of CO_2 in the final permeate stream. Case B with high permeable membrane in both stages yields the lowest membrane area requirement (up to 300% reduction) with almost no compromise in energy savings when lower purity of CO_2 (between 80% and 95%) is targeted at 90% recovery as seen in Fig. 10. Priorities between the savings in membrane area and energy requirements are made in consideration with the required purity and specific needs of the application such as lower footprint, minimal utility expenditure etc.

4. Conclusion

The current work explores possibilities and advantages of using membranes of different permeation properties in a two-stage cascade for post-combustion CO_2 capture. Two different classes of facilitated transport membranes with their performance validated in industrial conditions during field tests were used as the simulation basis. Both two-stage cascade with and without recycle stream were simulated for a CO_2 recovery target of up to 90% and CO_2 purity targets of 95%. Four different cases combining three membrane materials of different separation properties in different stages were analyzed. Without recycling, the maximum achievable CO_2 purity using two-stage cascade was limited to 89.43% using Case C (high permeability membrane in stage 1 and high selectivity membrane in stage 2) although high interstage compression was required. Higher CO_2 purity target was achieved using recycle stream in the two-stage process in all cases.

This study found that positioning of membranes with different properties in different stages influenced the performance of the system significantly. Processes with high permeable, low selective membrane in first stage coupled with a high selectivity, low permeable membrane in the second stage outperformed other cases in terms of low total membrane area requirement, low recycle ratio and low total energy requirement for a 90% recovery and >90% purity of CO_2. The base case of high selectivity, low permeable membrane in both stages (Case A) operates best only at lower purity requirements (<90%) albeit with high membrane area requirement. Case B offers the best solution in terms of footprint (lowest membrane area) for CO_2 lower purity targets (80 – 95%). The study establishes the potential of high permeability and low selectivity membranes as a bulk separator in first stage to act as feeder to a stage 2 comprising of a high selective membrane unit. The lower volumetric flow and relatively higher concentration of CO_2 in the feed supplied by membrane unit to stage 2 will prove beneficial for reducing the sizing of stage 2. High selective features of technologies used in stage 2 helps in obtaining high CO_2 purity targets, thereby increasing the efficiency of the overall process. The results obtained from this study also opens up potential for more such hybrid combinations of having membranes of different separation capabilities at different stages and combining membranes with high selective absorption/adsorption systems. Despite the permeance-selectivity trade-off often cited as the hurdle to the development and commercialization of interesting membrane and membrane materials, efforts should also focus on upscaling interesting membranes and deriving benefits of combining these upscalable membrane techologies that can synergistically reach the

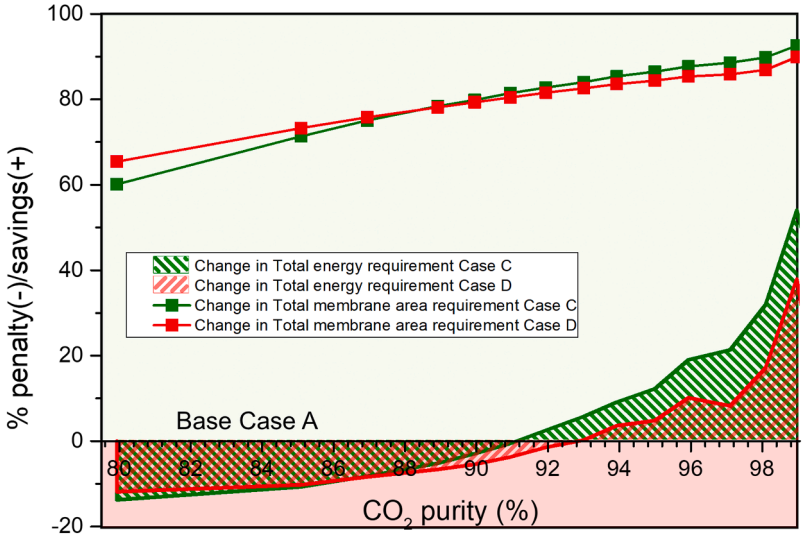

Fig. 9. Relative savings (positive values) or penalty (negative values) in Total membrane area/energy required by using Case C and Case D with respect to base Case A. Feed pressure in stage 1 = 1.7 bar; Interstage pressure = 1.7 bar; Permeate side: 0.1 bar vacuum in both stages; T = 60 °C.).

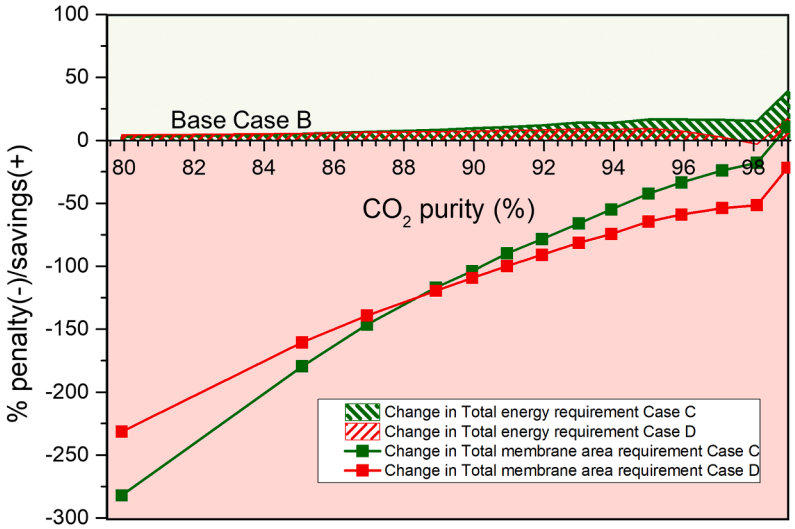

Fig. 10. Relative savings (positive values) or penalty (negative values) in Total membrane area/energy required by using Case C and Case D with respect to base Case B. Feed pressure in stage 1 = 1.7 bar; Interstage pressure = 1.7 bar; Permeate side: 0.1 bar vacuum in both stages; T = 60 °C.).

common goals in a multi-stage process for post combustion capture applications.

CRediT authorship contribution statement

Saravanan Janakiram: Conceptualization, Methodology, Investigation, Writing – original draft, Writing – review & editing. **Arne Lindbråthen:** Conceptualization, Validation, Investigation. **Luca Ansaloni:** Writing – review & editing. **Thijs Peters:** Writing – review & editing. **Liyuan Deng:** Conceptualization, Writing – review & editing, Supervision, Project administration, Funding acquisition.

Declaration of Competing Interest

The authors declare that they have no known competing financial interests or personal relationships that could have appeared to influence the work reported in this paper.

Acknowledgments

This work is a part of the FaT H2 project supported by the Research Council of Norway (No. 294533).

References

Ahmadi, M., Janakiram, S., Dai, Z., Ansaloni, L., Deng, L., 2018. Performance of mixed matrix membranes containing porous two-dimensional (2D) and three-dimensional (3D) fillers for CO2separation: a review. Membranes (Basel) 8, 50. https://doi.org/10.3390/membranes8030050.

R.W. Baker, Membrane Technology and Applications, 2004. https://doi.org/10.1016/S0376-7388(00)83139-7.

Belaissaoui, B., Willson, D., Favre, E., 2012. Membrane gas separations and post-combustion carbon dioxide capture: parametric sensitivity and process integration strategies. Chem. Eng. J. 122–132. https://doi.org/10.1016/j.cej.2012.09.012, 211–212.

Belaissaoui, B., Lasseuguette, E., Janakiram, S., Deng, L., Ferrari, M.C., 2020. Analysis of CO2 facilitation transport effect through a hybrid poly (Allyl amine) membrane: pathways for further improvement. Membranes (Basel) 10, 1–23. https://doi.org/10.3390/membranes10120367.

D'Alessandro, D.M., Smit, B., Long, J.R., 2010. Carbon dioxide capture: prospects for new materials. Angew. Chem. - Int. Ed. 49, 6058–6082. https://doi.org/10.1002/anie.201000431.

Dai, Z., Fabio, S., Giuseppe Marino, N., Riccardo, C., Deng, L., 2019a. Field test of a pre-pilot scale hollow fiber facilitated transport membrane for CO2 capture. Int. J. Greenh. Gas Control 86, 191–200. https://doi.org/10.1016/j.ijggc.2019.04.027.

Dai, Z., Deng, J., Ansaloni, L., Janakiram, S., Deng, L., 2019b. Thin-film-composite hollow fiber membranes containing amino acid salts as mobile carriers for CO2 separation. J. Memb. Sci. https://doi.org/10.1016/j.memsci.2019.02.023.

Deng, L., Hägg, M.B., 2010. Techno-economic evaluation of biogas upgrading process using CO2 facilitated transport membrane. Int. J. Greenh. Gas Control 4, 638–646. https://doi.org/10.1016/j.ijggc.2009.12.013.

Favre, E., 2007. Carbon dioxide recovery from post-combustion processes: can gas permeation membranes compete with absorption? J. Memb. Sci. 294, 50–59. https://doi.org/10.1016/j.memsci.2007.02.007.

Franz, J., Schiebahn, S., Zhao, L., Riensche, E., Scherer, V., Stolten, D., 2013. Investigating the influence of sweep gas on CO2/N2 membranes for post-combustion capture. Int. J. Greenh. Gas Control 13, 180–190. https://doi.org/10.1016/j.ijggc.2012.12.008.

Ghiat, I., Al-Ansari, T., 2021. A review of carbon capture and utilisation as a CO2 abatement opportunity within the EWF nexus. J. CO2 Util. 45, 101432 https://doi.org/10.1016/j.jcou.2020.101432.

Giordano, L., Roizard, D., Bounaceur, R., Favre, E., 2017. Evaluating the effects of CO2 capture benchmarks on efficiency and costs of membrane systems for post-combustion capture: a parametric simulation study. Int. J. Greenh. Gas Control. https://doi.org/10.1016/j.ijggc.2017.05.002.

Glenn Lipscomb, G., Sonalkar, S., 2004. Sources of non-ideal flow distribution and their effect on the performance of hollow fiber gas separation modules. Sep. Purif. Rev. 33, 41–76. https://doi.org/10.1081/SPM-120030236.

Grainger, D., Hägg, M.B., 2008. Techno-economic evaluation of a PVAm CO2-selective membrane in an IGCC power plant with CO2 capture. Fuel 87, 14–24. https://doi.org/10.1016/j.fuel.2007.03.042.

D. Grainger, Development of carbon membranes for hydrogen recovery, 2007. https://ntnuopen.ntnu.no/ntnu-xmlui/bitstream/handle/11250/248707/123275_FULLTEXT01.pdf?sequence=1&isAllowed=y.

Hägg, M.B., Lindbråthen, A., He, X., Nodeland, S.G., Cantero, T., 2017. Pilot demonstration-reporting on CO2 capture from a cement plant using hollow fiber process. Energy Proc. 114, 6150–6165. https://doi.org/10.1016/j.egypro.2017.03.1752.

Han, Y., Salim, W., Chen, K.K., Wu, D., Ho, W.S.W., 2019a. Field trial of spiral-wound facilitated transport membrane module for CO2 capture from flue gas. J. Memb. Sci. 575, 242–251. https://doi.org/10.1016/j.memsci.2019.01.024.

Han, Y., Wu, D., Ho, W.S.W., 2019b. Simultaneous effects of temperature and vacuum and feed pressures on facilitated transport membrane for CO2/N2 separation. J. Memb. Sci. 573, 476–484. https://doi.org/10.1016/j.memsci.2018.12.028.

He, X., Fu, C., Hägg, M.B., 2015. Membrane system design and process feasibility analysis for CO2capture from flue gas with a fixed-site-carrier membrane. Chem. Eng. J. 268, 1–9. https://doi.org/10.1016/j.cej.2014.12.105.

He, X., Lindbråthen, A., Kim, T.J., Hägg, M.B., 2017. Pilot testing on fixed-site-carrier membranes for CO2 capture from flue gas. Int. J. Greenh. Gas Control 64, 323–332. https://doi.org/10.1016/j.ijggc.2017.08.007.

Helberg, R.M.L., Torstensen, J., Dai, Z., Janakiram, S., Chinga-Carrasco, G., Gregersen, Ø.W., Syverud, K., Deng, L., 2021. Nanocomposite membranes with high-charge and size-screened phosphorylated nanocellulose fibrils for CO2 separation. Green Energy Environ. 6, 585–596. https://doi.org/10.1016/j.gee.2020.08.004.

Ho, M.T., Allinson, G.W., Wiley, D.E., 2008. Reducing the cost of CO2 capture from flue gases using membrane technology. Ind. Eng. Chem. Res. 47, 1562–1568. https://doi.org/10.1021/ie070541y.

Janakiram, S., Ahmadi, M., Dai, Z., Ansaloni, L., Deng, L., 2018. Performance of nanocomposite membranes containing 0D to 2D nanofillers for CO2 separation: a review. Membranes (Basel) 8. https://doi.org/10.3390/membranes8020024.

Janakiram, S., Yu, X., Ansaloni, L., Dai, Z., Deng, L., 2019. Manipulation of fibril surfaces in nanocellulose-based facilitated transport membranes for enhanced CO2 capture. ACS Appl. Mater. Interfaces 11, 33302–33313. https://doi.org/10.1021/acsami.9b09920.

Janakiram, S., Ansaloni, L., Jin, S.-.A., Yu, X., Dai, Z., Spontak, R.J., Deng, L., 2020a. Humidity-responsive molecular gate-opening mechanism for gas separation in ultraselective nanocellulose/IL hybrid membranes. Green Chem. 22, 3546–3557. https://doi.org/10.1039/D0GC00544D.

Janakiram, S., Luis Martín Espejo, J., Yu, X., Ansaloni, L., Deng, L., 2020b. Facilitated transport membranes containing graphene oxide-based nanoplatelets for CO2 separation: effect of 2D filler properties. J. Memb. Sci. 616, 118626 https://doi.org/https://doi.org/10.1016/j.memsci.2020.118626.

Janakiram, S., Santinelli, F., Costi, R., Lindbråthen, A., Nardelli, G.M., Milkowski, K., Ansaloni, L., Deng, L., 2020c. Field trial of hollow fiber modules of hybrid facilitated transport membranes for flue gas CO2 capture in cement industry. Chem. Eng. J., 127405 https://doi.org/https://doi.org/10.1016/j.cej.2020.127405.

Janakiram, S., Martín Espejo, J.L., Høisæter, K.K., Lindbråthen, A., Ansaloni, L., Deng, L., 2020d. Three-phase hybrid facilitated transport hollow fiber membranes for enhanced CO2 separation. Appl. Mater. Today 21, 100801 https://doi.org/https://doi.org/10.1016/j.apmt.2020.100801.

Kim, T.J., Vrålstad, H., Sandru, M., Hägg, M.B., 2013. Separation performance of PVAm composite membrane for CO2 capture at various pH levels. J. Memb. Sci. 428, 218–224. https://doi.org/10.1016/j.memsci.2012.10.009.

Li, D., Wang, R., Chung, T.S., 2004. Fabrication of lab-scale hollow fiber membrane modules with high packing density. Sep. Purif. Technol. 40, 15–30. https://doi.org/10.1016/j.seppur.2003.12.019.

Low, B.T., Zhao, L., Merkel, T.C., Weber, M., Stolten, D., 2013. A parametric study of the impact of membrane materials and process operating conditions on carbon capture from humidified flue gas. J. Memb. Sci. 431, 139–155. https://doi.org/10.1016/j.memsci.2012.12.014.

Mulder, M., 1996. Basic Principles of Membrane Technology, 5. Kluwer Academic Publisers. https://doi.org/10.1016/0376-7388(92)85058-Q.

Park, H.B., Kamcev, J., Robeson, L.M., Elimelech, M., Freeman, B.D., 2017. Maximizing the right stuff: the trade-off between membrane permeability and selectivity. Science (80-.) 356. https://doi.org/10.1126/science.aab0530 eaab0530.

Psarras, P.C., Comello, S., Bains, P., Charoensawadpong, P., Reichelstein, S., Wilcox, J., 2017. Carbon capture and utilization in the industrial sector. Environ. Sci. Technol. 51, 11440–11449. https://doi.org/10.1021/acs.est.7b01723.

Salim, W., Vakharia, V., Chen, Y., Wu, D., Han, Y., Ho, W.S.W., 2018. Fabrication and field testing of spiral-wound membrane modules for CO2 capture from flue gas. J. Memb. Sci. 556, 126–137. https://doi.org/10.1016/j.memsci.2018.04.001.

Sandru, M., Kim, T.J., Capala, W., Huijbers, M., Hägg, M.B., 2013. Pilot scale testing of polymeric membranes for CO2 capture from coal fired power plants. Energy Proc. 37, 6473–6480. https://doi.org/10.1016/j.egypro.2013.06.577.

Shao, P., Dal-Cin, M.M., Guiver, M.D., Kumar, A., 2013. Simulation of membrane-based CO2 capture in a coal-fired power plant. J. Memb. Sci. 427, 451–459. https://doi.org/10.1016/j.memsci.2012.09.044.

Wang, Y., Zhao, L., Otto, A., Robinius, M., Stolten, D., 2017. A review of post-combustion CO2 capture technologies from coal-fired power plants. Energy Proc. 114, 650–665. https://doi.org/10.1016/j.egypro.2017.03.1209.

White, L.S., Wei, X., Pande, S., Wu, T., Merkel, T.C., 2015. Extended flue gas trials with a membrane-based pilot plant at a one-ton-per-day carbon capture rate. J. Memb. Sci. 496, 48–57. https://doi.org/10.1016/j.memsci.2015.08.003.

Yang, D., Wang, Z., Wang, J., Wang, S., 2009. Potential of two-stage membrane system with recycle stream for CO2 capture from postcombustion gas. Energy Fuels 23, 4755–4762. https://doi.org/10.1021/ef801109p.

Zhao, L., Riensche, E., Blum, L., Stolten, D., 2010. Multi-stage gas separation membrane processes used in post-combustion capture: energetic and economic analyses. J. Memb. Sci. 359, 160–172. https://doi.org/10.1016/j.memsci.2010.02.003.

Zhaurova, M., Soukka, R., Horttanainen, M., 2021. Multi-criteria evaluation of CO2 utilization options for cement plants using the example of Finland. Int. J. Greenh. Gas Control 112, 103481. https://doi.org/10.1016/j.ijggc.2021.103481.